

## INTERSTELLAR POLARIZATION IN THE SOUTHERN MILKY WAY

ELSKE VAN P. SMITH\*

Harvard College Observatory

*Received February 3, 1956; revised March 18, 1956*

## ABSTRACT

Polarization observations are reported for over two hundred stars in the southern Milky Way between longitudes  $200^\circ$  and  $350^\circ$ . Analysis of these and other data for the north seems to confirm the model of a polarizing medium where the elongated particles are aligned perpendicular to the spiral-arm axis. Light from stars in the Sagittarius or Perseus arms appears to acquire most of its polarization from dust clouds lying in the Orion arm. The amount of polarization per unit extinction is lower in the southern Milky Way than in the northern. Although the possibility of a difference in the optical properties of the grains is not ruled out, an alternative hypothesis seems preferable. We suggest that the particles are more rigidly aligned in the center of the spiral arm, through which the line of sight passes when we look northward, than at the periphery of the arm. Finally, we discuss in some detail individual regions in the southern Milky Way, including Vela, Carina, the Coal Sack in Crux, and Scorpius. The Scorpius region, in particular, shows that local structure may considerably distort the general effect.

## I. INTRODUCTION: INSTRUMENTATION AND THE POLARIZATION SYSTEM

All previous observations of interstellar polarization have been carried out in the Northern Hemisphere, so that a large segment of our Galaxy has remained unexplored. The southern Milky Way is of particular interest, since here the field of view covers the inner edge of the Orion arm and the whole of the Sagittarius arm; one can also penetrate to the second inner spiral arm. In an attempt to fill this gap, more than two hundred stars between  $200^\circ$  and  $350^\circ$  longitude were observed for polarization at the Boyden Station of Harvard Observatory in South Africa.

The greater part of the data was obtained with the 60-inch Rockefeller reflector. A calcite crystal<sup>1</sup> served as the polarizing analyzer and was mounted in a photoelectric polarimeter used in conjunction with the amplifier of the Linnell-King photometer. Initial plans included a seeing-compensation scheme which utilized both rays emerging from the calcite, but these plans had to be abandoned because of instrumental difficulties. Hence the observations discussed here were made by the use of only the ordinary ray.

The technique of observation and reduction resembles that described by Hiltner (1951), with some modifications. To measure the amount of polarization, the amplifier gain was increased by a factor of approximately 10 over that required for the total intensity of the star. Since the dark current was far below the zero reading of the recorder tape, it was possible only to read differences in intensity at complementary positions of the calcite crystal. This procedure necessitated separate readings to obtain the total intensity; these were made at the beginning and end of each set of observations. As in Hiltner's procedure, master sine-curves were used in the reductions.

Since the mirror of the 60-inch telescope has no central hole, the polarimeter was attached at the Newtonian focus. A combination of a second flat mirror, mounted normal to the Newtonian, and a set of tilted glass disks partially compensated for elliptical polarization introduced by the Newtonian flat. Although this device considerably reduced the instrumental polarization, nevertheless some remained, as was shown by observations of nearby stars that could be assumed to be unpolarized. To correct for this instrumental polarization, it became necessary to establish an error-free system of polarization, which we obtained from measurements made with the 13-inch Boyden

\* Now at Sacramento Peak Station of Harvard Observatory, Sunspot, New Mexico.

<sup>1</sup> Generously donated by the Polaroid Corporation, Cambridge, Mass.

refractor. The 13-inch polarimeter consisted simply of a rotating piece of polaroid mounted in place of the filter holder of a photometer, kindly loaned by the Washburn Observatory South African Expedition. A depolarizer in front of the 1P21 photomultiplier eliminated the problem of sensitivity changing with the plane of vibration. Careful observations of unpolarized, nearby stars confirmed the absence of any instrumental polarization. However, the position angles of the plane of vibration on the 13-inch, or Smith, polarization system differ by  $-2^\circ$  from those of Hall (Hall and Mikesell 1950; Hall, unpublished) and of Hiltner (1951, 1954), as determined from data on stars measured in common with one or another of the northern observers. The zero point of the 13-inch system was carefully checked, and no cause of the difference could be found. No such systematic difference appears when amounts of polarization are compared. The 60-inch observations were reduced to the Smith system by means of calibration-curves derived from a comparison of 60-inch data with 13-inch data for the same stars.

TABLE 1  
DISPERSIONS IN COMPARISONS BETWEEN DATA OF SMITH (EPS),  
HALL (JSH), AND HILTNER (WAH)

	$\sigma_\theta$			$\sigma_p$		
	JSH	WAH	EPS	JSH	WAH	EPS
EPS ( $P < 0^m.050$ )	12°3	4°2		0 <sup>m</sup> .0083	0 <sup>m</sup> .0034	
EPS ( $P > 0^m.050$ )	5 3	3 5		0125	0046	
JSH		3 3	4°5		0093	0 <sup>m</sup> .0082
13-in ( $P < 0^m.050$ )	7 1}	2 6	{4 0	{0101}	0 0048	{0055
13-in ( $P > 0^m.050$ )	5 5}		{2 5	0 0132}		{0 0044

In view of the method of calibration, a calculation of probable errors in the observations would have little meaning, but we may estimate that they are, in general, less than  $\pm 0.004$  mag. for individual values of the amount of polarization,  $P_{\Delta m}$ , and less than  $\pm 4^\circ$  in position angle,  $\theta$ . An additional measure of the accuracy of the final values of the derived polarizations lies in the dispersions found from comparisons with other systems. A correction of  $-2^\circ$  was applied to the residuals in position angle used in computing the dispersions which compare the Smith observations with those of Hall or Hiltner. Hall's position angles required a conversion from the plane of polarization to the plane of vibration by the addition of  $90^\circ$ . Similarly, his percentage polarization had to be changed into magnitude increments by the relation

$$P_{\%} = 46.05 P_{\Delta m},$$

to bring his values into the same units as those used by Smith and Hiltner. Table 1 lists the dispersions in the comparisons among the three sets of observations. The Smith observations represent the finally adopted values of the polarization. Generally, these consist of the 60-inch data, but weighted means were used when 13-inch observations were also available. The first and second rows give the simple comparisons of Smith's data with those of Hall or Hiltner, separated into small and large amounts of polarization. The third row compares Hall's data with those of Hiltner and Smith for stars observed in common by all three. The Hall-Smith comparisons are clearly similar to the Hall-Hiltner dispersions for the same stars. Since the 13-inch data actually define the Smith system, separate comparisons with the observations of Hall and Hiltner are of interest. Too few stars were observed in common with Hiltner to permit a breakdown

into small and large polarizations. The 13-inch Smith figures actually refer to comparison between 13-inch and reduced 60-inch observations and are therefore an indication of the success of the calibrations. Table 1 shows that the dispersion in the comparisons of Smith's data with those of Hiltner is considerably less than with those of Hall. In all probability we may attribute this to the quality of the skies under which the respective observations were obtained.

## II. THE CATALOGUE

Table 2 presents the spectral, photometric, and polarimetric data for all the stars observed.

Column 1 gives the *HD* or *HDE* number of the star.

Columns 2 and 3 list the galactic co-ordinates of the star, as referred to the Lund pole (Ohlson 1932).

Column 4 notes the spectral type on the MK system (Johnson and Morgan 1953) when it is available (Sharpless 1952; Hiltner 1954; Morgan, Code, and Whitford 1955; Hoffleit, unpublished; Houck, unpublished); otherwise *HD* spectral types are given.

Columns 5 and 6 give, respectively, the magnitude to a tenth on the *V* system of Johnson and Morgan (1951) and the color on the *C*<sub>1</sub> system of Stebbins, Huffer, and Whitford (1940). When more than one photoelectric magnitude or color (Oosterhoff 1951; Bok and van Wijk 1952; Sharpless 1952; Hiltner 1954; Morgan, Code, and Whitford 1955; Hoffleit, unpublished; Houck, unpublished) was available for a given star, the mean is listed. Colors from the Cape Zone photographic catalogue (Jackson and Stoy 1954, 1955) were also included in the mean, as the accuracy seems to be comparable to that obtained from photoelectric equipment. If no photoelectric magnitude was known, the magnitude given is that converted to the *V* system from the Cape or *HD* catalogues.

Column 7 gives the color excess,  $E_1$ , determined on the basis of the Morgan, Harris, and Johnson list (1953) of normal colors.

Column 8 lists the approximate distance modulus, where the absolute magnitude is generally taken from the published table of Morgan and Keenan (1951), and the visual absorption is given by the relation  $A_v = 6.1 E_1$  (Morgan, Harris, and Johnson 1953).

Columns 9–12 give the polarimetric data. The percentage polarization,  $P_{\%}$ , derives from the observed magnitude increment,  $P_{\Delta m}$ , by  $P_{\%} = 46.05 P_{\Delta m}$ . The position angle of the plane of vibration is referred to both the equatorial and the galactic co-ordinate system, which are denoted by  $\theta_E$  and  $\theta_G$ , respectively. Values which are less certain than the majority, as discussed in the first section, are indicated by the following code: a period (.) denotes an uncertainty of 0<sup>m</sup>005–0<sup>m</sup>010 in  $P_{\Delta m}$  and 5°–10° in  $\theta$ ; a colon (:) signifies an uncertainty of 0<sup>m</sup>010–0<sup>m</sup>020 in  $P_{\Delta m}$  and 10°–20° in  $\theta$ ; quantities followed by a double colon (::) are uncertain by more than 0<sup>m</sup>020 or 20°.

Column 13 gives the number of observations of each star. Figures in parentheses indicate observations with the 13-inch; others refer to the 60-inch observations.

## III. RELATION OF POLARIZATION TO SPIRAL STRUCTURE

Figure 1 illustrates the projected space distribution, in galactic co-ordinates, of the maximum of the electric vector of polarized starlight between longitudes 210° and 360°. One notes that the maximum of the electric vector has a preferential direction parallel to the galactic equator, as was already found in the north by Hall and Mikesell (1950) and by Hiltner (1951). Superimposed on this general phenomenon are important regional variations, which appear to be correlated with the orientation of the axes of spiral arms to the line of sight. This correlation is such that when we are looking transverse to a spiral arm, i.e., the axis of the arm crosses the line of sight, the maximum of the electric vector is far more uniformly aligned than it is when we are looking along a spiral arm. The region between  $l = 265^\circ$  and  $l = 310^\circ$  corresponds to the segment of the Milky Way

TABLE 2

## POLARIZATION AND RELATED DATA OF SOUTHERN STARS

HD	$l$	$b$	Sp	$m_V$	$C_1$	$E_1$	$m_0-M$	$P_{\%}$	$P_{\Delta m}$	$\theta_E$	$\theta_G$	No.
35149	166.7	-16.4	B1 V	4.9	-.20	+.04	7.9	0.4	.008	70°	10°	2
36629	175.6	-18.0	B2 V	7.6	-.13	+.10	9.6	1.8	.040	98	36	2
36958	175.9	-18.1	B3	7.4	-.18	+.04	8.4	1.3	.028	39	156	3
37041	176.7	-17.9	O9.5 Vp	5.1	-.16	+.11	8.6	0.5	.011	71	9	2
37061	176.7	-17.8	B1 V	6.9	0.00	+.24	8.6	1.3	.028	60	178	2
42051	181.5	-11.4	B3	8.9	+.01	+.23		1.7	.038	106°	43°	2
259597	171.2	+ 1.3	B0.5:V:nne	8.5	-.16	+.09	11.4	1.1	.023	70	8	2
46769	178.0	- 1.8	B3s	5.6	-.12	+.10		1.2	.025	122	60	2
47129	173.6	+ 1.2	O8	6.0	-.12	+.16	9.7	1.0	.022	155	93	2
47398	175.1	+ 0.8	B2	8.3	-.13	+.10		1.3	.029	160	98	2
51354	165.3	+10.9	B3ne	7.0	-.22	0.00		0.9	.020	139°	75°	2
52559	176.9	+ 6.3	B2s	6.4	-.12	+.11		1.1	.023	63	1	2
54662	191.9	+ 0.6	O6	6.1	-.15	+.14	10.3	0.8	.017	142	81	2
61709	213.6	- 3.5	B1	8.2	-.04	+.20		1.7	.038	126	67	3
61827	214.7	- 4.0	O8:	7.7	+.13	+.41	9.9	1.9	.041	2	125	4(2)
62150	214.9	- 3.9	B3 Ia	7.7	+.10	+.32	12.7	2.4	.053	143°	84°	4(1)
-324348	213.2	- 2.0	B	9.0	+.37	+.63		2.8	.061	123	65	3
62844	215.0	- 3.0	B0	8.1	+.21	+.47		1.7	.038	4	125	2
63804	216.4	- 2.7	B	7.6	+.51	+.77		2.5	.055	23	145	2
68450	222.1	- 1.2	B0 II	6.5	-.14	+.12	11.8	-	-	-	-	2
68761	222.0	- 0.9	B0.5 III	6.6	-.17	+.08	10.5	<0.4	<.008	-	-	3
69106	222.1	- 0.5	B0.5 II	7.2	-.17	+.08	11.9	-	-	-	-	4
71304	229.4	- 3.1	O9 III?	8.2	+.12	+.39	11.5	1.3	.028	36°	163°	2
73882	227.9	+ 1.3	O8(V)	7.3	+.06	+.34	9.9	1.8	.040	163	112	5(3)
75860	231.9	+ 0.9	B1.5 Iab	7.7	+.23	+.47	11.3	1.7	.037	138	89	3
76968	237.9	- 2.9	B0 II	7.1	-.09	+.17	11.3	1.2	.026	178°	130°	4
77581	230.9	+ 4.6	B0.5 Ib	6.9	+.10	+.35	10.8	3.5	.077	80	33	5(3)
77718	235.4	+ 0.6	B2	8.7	+.19	+.42		2.7	.059	20	154	3
78785	235.8	+ 1.5	B2	8.7	+.14	+.37		4.5	.097	5	140	2
78958	233.8	+ 3.3	B0.5 II	9.1	+.20	+.45	11.6	3.1	.068	91	46	3
79573	239.1	- 0.6	WC6	10.8				5.5	.119	156°	112°	3
80077*	239.3	- 0.1	B2 Iape	7.7	+.53	+.76	10.1	3.8	.082	147	103	3
298298	240.3	- 2.9	B1 Vpe	9.1	+.03	+.27	10.7	1.9	.042	164	119	2
298310*	240.2	- 1.1	B0					2.5	.055	164	120	2
298369	240.8	- 0.4	B1 Vp	9.5	+.05	+.29	10.9	1.5	.032	162	119	3
298387	241.6	- 1.8	B2 V	10.3	-.07	+.16	11.9	1.7	.036	139°	96°	2
298383	241.8	- 1.3	A0 Ib	9.7	+.29	+.41	12.2	5.1	.111	148	105	3
81370	242.0	- 1.4	B0 IV:	8.8	-.09	+.17	12.0	2.5	.054	128	85	2
298377	241.6	- 0.8	B1 IV:	10.4	+.01	+.25	12.7	2.3	.050	140	98	3
83043	243.9	- 1.0	B1 V:pe	8.5	-.12	+.12	11.0	1.7	.036	160	120	2

TABLE 2 (Continued)

HD	$\ell$	b	Sp	$m_v$	$C_1$	$E_1$	$m_{O-M}$	$P\%$	$F_{\Delta m}$	$\theta_E$	$\theta_G$	No.
83597	244.3	- 1.0	B1 Vpe	9.3	-0.8	+0.16	11.5	1.3	.029	157°	117°	2
300167	244.9	- 0.8	B2	8.7	+0.40	+0.63		1.1	.024	112	73	3
300214	244.6	- 0.4	B	8.6	+0.41	+0.67		5.2	.112	146	108	2(2)
84567	230.0	+18.1	B2	6.4	-0.20	+0.03		0.8	.020	71	30	4(3)
84861	245.6	- 0.2	B2	8.7	+0.14	+0.37		3.4	.074	154	116	2
90615	252.0	+ 0.4	B0 II	8.2	-0.01	+0.25	11.9	1.1	.024	133°	103°	2
90706	252.2	+ 0.3	B3 I:	7.2	+0.09	+0.31	11.6	2.7	.059	151	121	6(3)
90831	252.2	+ 0.4	B2 III	9.4	+0.07	+0.30	11.7	1.3	.028	150°	120°	3
90832	252.2	+ 0.3	B1 III	9.1	+0.04	+0.28	11.7	1.2	.027	150°	120°	4
300774	252.2	+ 0.6	B3	9.7	+0.21	+0.43		2.5	.054	165°	136°	2
91824	253.4	+ 0.3	O7	7.9	-0.16	+0.13	12.1:	1.8	.038	107°	79°	3
91850	253.4	+ 0.3	B1 IV:	9.2	-0.04	+0.20	11.8	2.8	.060	108	80	3
91943	253.5	+ 0.2	B0.5 Ib	6.8	-0.10	+0.15	11.9	1.2	.025	110	82	6(3)
91969	253.6	+ 0.2	B0 Ib	6.6	-0.13	+0.13	11.8	1.8	.038	111	83	5(3)
91983	253.6	+ 0.1	B1 III	8.6	-0.11	+0.13	12.1	1.9	.042	127	99	2
92007	253.6	+ 0.2	B0 II	8.1	-0.09	+0.17	12.3	1.2	.025	123°	95°	2
92044	253.6	+ 0.1	B0.5 II	8.3	-0.06	+0.19	12.3	1.3	.028	142	114	3
92060	253.5	+ 0.4	B2	8.7	+0.06	+0.29		3.2	.070	122	94	5
92206*	253.9	- 0.1	O7	7.7	-0.07	+0.22	11.4	2.9	.062	87	59	6
92207*	253.8	- 0.2	A0 Ia	5.5			11.2:	3.2	.070	112	84	6(3)
92420	253.7	+ 0.7	B2	9.0	+0.01	+0.24		2.8	.060	96°	69°	6
92740	254.8	- 0.7	WN7	6.4	-0.10			2.2	.048	100	73	2
93131	255.3	- 1.0	WN7	6.5	-0.16			2.9	.064	100	74	2
93206	255.4	- 0.9	B0 Ib:	6.5	-0.07	+0.19	11.3	2.9	.064	112°	86°	2
93342	255.2	- 0.3	B0 III:	9.0	+0.19	+0.45	10.7:	1.4	.031	70°	44°	2
93403	255.2	- 0.3	O5 (f)	7.3	-0.02	+0.27:		2.2	.047	100°	74°	5
93795	255.6	- 0.2	A0 Ia	9.0	+0.28	+0.40	13.6	2.2	.048	95°	70°	3
93890	255.4	+ 0.4	B	9.1	+0.27	+0.53		<0.5	<.010	-	-	2
94369	255.5	+ 1.1	B1 I	7.4	+0.01	+0.25	12.4	1.2	.025	142	118	3(3)
94909	255.7	+ 2.0	B0 Ib	7.3	+0.10	+0.36	11.1	4.7	.103	117	93	5
96248	257.6	+ 0.3	B1 Iab	6.6	-0.03	+0.21	11.8	0.9	.020	132°	110°	5(3)
96261	257.6	+ 0.4	B1 Ib	7.6	-0.04	+0.20	12.4	1.7	.037	112	90	2
96670	257.9	+ 0.4	O8	7.4	-0.06	+0.22	10.7:	1.7	.036	177	156	7
96880	257.9	+ 1.0	B1 Ib	7.6	+0.10	+0.34	11.5	2.3	.049	60	39	4(3)
97222	258.4	+ 0.3	B0 II:	8.7	-0.03	+0.23	12.5:	1.3	.028	118	98	3
97253	258.5	+ 0.1	O6	7.0	-0.06	+0.23:		1.0	.022	143°	123°	5
97848	258.5	+ 1.5	O9 IV	8.7	-0.14	+0.13	12.7	0.7	.016	86:	66:	2
97950*	259.5	- 0.6	WN5 + O	9.0	+0.32			1.2	.026	130	110	2
97966	258.7	+ 1.1	O7.5	8.9	-0.12	+0.17	12.7:	0.5	.011	94:	73:	2
98733	259.6	+ 0.7	B1 Ib	8.0	-0.05	+0.19	12.8	1.0	.022	70°	52°	2
99546	260.1	+ 1.6	O8	8.3	-0.15	+0.13	12.2	1.5	.032	120°	103°	2
99953	261.6	- 2.2	B2 Ia	6.5	+0.01	+0.24	12.0	2.0	.044	103	86	5(3)
100099	261.7	- 2.5	O9.5 V†	8.1	-0.09	+0.18	11.1	1.1	.023	108:	92:	3
100199	261.6	- 1.6	B1 Ibp	8.1	-0.11	+0.13	13.3	<0.5	<.010	-	-	3
102997	263.6	0.0	B5 Ia	6.1	+0.01	+0.20	12.4	1.2	.026	74°	62°	5

TABLE 2 (Continued)

HD	$\ell$	b	Sp	$m_V$	$C_1$	$E_1$	$m_0-M$	$P_g$	$P_{\Delta m}$	$\theta_E$	$\theta_G$	No.
103779	264.5	- 1.2	B0.5 Ib	7.2	-.15	+.10	12.6	0.7	.015	80°	69°	4(3)
104631	265.0	0.0	B1 II	6.8	-.09	+.15	11.0	0.4	.008	69	59	3
104705	265.1	- 0.5	B0.5 III	7.8	-.14	+.11	11.5	0.4	.008	-	-	3
110360	269.6	+ 1.9	O7	9.4	-.07	+.22	13.1	1.4	.030	90	89	2
110432*	269.6	- 0.5	B2nne	5.4	-.04	+.19	7.0	2.0	.044	76	75	5(3)
110639	269.8	+ 1.2	B1 Ib - II	8.4	+.19	+.43	11.3	3.5	.075	89°	89°	2
110660	269.8	- 1.5	B1 V	10.0	+.12	+.36	11.0	2.9	.063	72	72	1
110863	270.0	+ 2.0	B1 Vp	9.0	+.04	+.28	10.5	2.9	.062	93	93	3
110984	270.1	+ 1.4	B0 IV	9.0	+.11	+.37	10.9	5.3	.115	88	88	3(3)
111124	270.2	- 0.4	B0	9.1	+.20	+.46		1.2	.025	22	23	2
111193	270.2	+ 2.3	B0	8.0	-.03	+.23		3.4	.073	80°	80°	4(3)
311999*	270.5	+ 1.0	O9.5 IV	10.9	+.12	+.44	12.7	2.9	.062	94	95	2
111579	270.6	+ 1.3	B2	9.2	+.19	+.42		5.5	.120	103°	104°	3
312052	270.6	- 0.7	B	11.5	+.12	+.38		2.6	.056	57	58	2
312051	270.7	- 0.6	B	11.3	+.22	+.48		3.0	.065	53	54	2
112027	271.0	+ 1.5	B2	9.2	+.16	+.39		2.4	.052	53°	55°	2
312155	271.3	0.0	B0					1.6	.035	43	45	2
112272	271.2	- 1.8	B0.5 Ia	7.4	+.25	+.50	11.4	1.1	.023	55	57	4(3)
312259	271.6	+ 0.9	B	10.6	+.43	+.69		5.5	.119	90	93	3
312258	271.7	+ 0.9	B	10.4	+.47	+.73		6.4	.140	88	91	3
112784	271.7	+ 1.9	O9.5 III	8.3	-.11	+.17	12.3	1.8	.040	84°	87°	3
112953	271.9	+ 1.5	B2	9.1	+.24	+.47		4.6	.099	81	84	2
113034	271.8	+ 0.6	B1 I:	9.3	+.37	+.61	12.1	4.6	.099	80	83	4(3)
113163	272.1	+ 1.7	B5 IV	7.8	0.00	+.19	8.8	2.4	.052	88	92	6(3)
113422	272.2	+ 0.7	B1 Ia	8.3	+.26	+.50	12.3	5.7	.125	82	86	5(3)
312256	272.3	+ 0.8	B	9.8	+.24	+.50		4.0	.088	100°	104°	2
113511	272.1	- 1.6	B0 III:	9.1	+.08	+.34	11.5	1.9	.041	70°	74°	2
113754	272.4	- 0.7	B0	9.5	+.19	+.45		4.6	.100	71	76	2
114011	272.8	+ 1.3	B1.5 Ia(+)	9.3	+.24	+.51	13.2+	1.1	.025	-	-	3
114122	272.7	- 0.4	B0	8.7	+.14	+.40		2.7	.059	84	89	2
114340	273.2	+ 2.6	B1 Ia+	8.2	+.12	+.36	13.0+	5.0	.108	74°	80°	3
114341	273.2	+ 2.2	B0 III: nm	8.6	+.05	+.31	11.2:	2.3	.050	78	84	2
114478	273.0	- 0.5	B1 II	8.8	+.10	+.34	11.8	1.6	.035	71	77	2
115363	273.6	- 1.4	B1 Ia+	7.8	+.15	+.39	12.4+	3.1	.067	58	65	2
115704	274.1	+ 0.2	B0	8.2	+.08	+.34		3.5	.075	71	79	3
115746	273.8	- 1.2	B2	9.4	+.03	+.26		2.3	.050	60°	68°	2
116119	274.4	+ 0.2	B9 I	8.1	+.21	+.35	12.2	2.9	.064	76	84	3
117111	274.5	- 3.4	B1 Vpe	7.6	-.09	+.15	9.9	1.4	.030	70	80	3(3)
117707	275.0	- 3.2	B0.5 I	9.5	+.13	+.38	13.7	2.4	.052	58	68	2
122324	280.7	+ 4.9	B0	9.1	+.08	+.34		4.5	.097	81	98	2
122450	279.8	+ 1.5	B0	9.3	+.08	+.34		1.2	.027	70°	87°	2
122879	280.0	+ 1.2	B0 Iab	6.4	-.08	+.18	11.8	1.6	.035	70	87	5(3)
123056	279.9	+ 0.5	O9.5 V	8.2	-.08	+.18	11.2	1.6	.035	66	84	5
124909	281.0	- 0.4	B2	9.2	-.01	+.22		1.3	.029	55	75	2
125206	281.2	- 0.6	B2	8.0	-.02	+.21		2.2	.047	58	78	3(3)

TABLE 2 (Continued)

HD	$l$	$b$	Sp	$m_V$	$C_1$	$E_1$	$m_o-M$	$F_{\%}$	$F_{\Delta m}$	$\theta_E$	$\theta_G$	No.
125241	281.3	- 0.4	O9 I	8.4	+0.04	+0.31	13.0	2.0	.044	67°	87°	2
126940	282.6	- 0.5	B2	9.5	+0.09	+0.32		4.7	.102	80	103	2
134959*	288.2	- 2.0	B0	8.1	+0.33	+0.59		6.0	.130	66	98	6
135591	287.8	- 3.4	O9 Ib	5.3	-0.20	+0.07	10.9	0.7	.016	43	76	2
136003	290.3	+ 0.1	B1	6.8	-0.05	+0.19		2.9	.063	66	99	5(3)
136239	288.8	- 2.6	B2 Ia+	8.0	+0.34	+0.57	12.5+	4.6	.100	67°	100°	6(3)
136488	287.1	- 5.5	WC8	9.4	0.00			2.9	.064	66	100	2
138764	324.2	+35.0	B8s	5.1	-0.14	+0.01		0.6	.014	72	118	5(3)
142468	295.6	- 1.6	B0	8.0	+0.13	+0.39		2.3	.050	45	86	5
142565	295.7	- 1.8	B0 Ib	9.0	+0.08	+0.34	12.9	1.9	.042	40	81	2
142634	295.7	- 1.8	B0(II)p	9.0	+0.18	+0.44	11.5:	2.6	.057	55°	96°	3
142775	295.7	- 1.8	B2	9.3	+0.20	+0.43		1.9	.041	35	76	2
142983	324.4	+27.3	B3n	4.9	-0.13	+0.09		0.9	.020	122	170	2
144969	301.0	+ 1.0	B0.5 Ia	8.4	+0.37	+0.62	11.6	3.0	.065	27	70	1
144970	300.8	+ 0.8	B0	9.9	+0.27	+0.53		2.3	.051	45	88	1
145664	298.8	- 2.0	B2	8.4	+0.03	+0.26		3.7	.081	52°	96°	5
145794	298.5	- 2.5	B2	8.8	-0.02	+0.21		1.6	.035	34	78	2
145846	299.0	- 2.1	B2 Vpe	9.0	+0.04	+0.27	10.0	3.6	.079	52	96	2
146919	299.1	- 3.2	B1.5 Ia	8.7	+0.14	+0.38	13.4	3.4	.073	32	77	5
147049	299.4	- 3.0	B2	7.7	+0.01	+0.24		2.3	.050	43	89	3(3)
147331	299.8	- 3.0	B0 Ia	8.8	-0.01	+0.25	14.3	2.0	.043	39°	85°	2
147421	299.2	- 3.8	B2	9.0	-0.11	+0.12		2.5	.054	59°	105°	3
147888	321.5	+16.4	B3	6.5	+0.01	+0.23		2.8	.061	52	101	6(4)
147889	320.8	+15.7	B3	7.9	+0.27	+0.49		3.2	.069	175	44	7(3)
147932	321.6	+16.4	A	7.0				2.5	.055	58	107	5(3)
147933	321.6	+16.3	B5n	4.6	-0.03	+0.16		2.3	.051	47°	96°	3(3)
148184	325.8	+19.3	B3e	4.5	-0.01	+0.21		1.8	.039	113	164	1
148546	311.1	+ 5.9	O9.5I	7.8	-0.02	+0.25	12.8	2.0	.043	6	53	2
150475	312.9	+ 4.2	O8.5	8.8	0.00	+0.28	11.6	0.7:	.016:	71:	120:	5
151397	312.1	+ 2.0	B2	9.9	-0.02	+0.21		1.8	.038	5	55	3
151932	310.9	+ 0.2	WN8	6.5	0.00			1.2	.025	43::	94::	1
151985	314.0	+ 2.6	B2	3.4	-0.22	+0.01		0.5	.010	25	76	(2)
152408	311.9	+ 0.3	O8 fp	5.8	-0.06	+0.22	9.2	0.7	.016	39	90	3(2)
152667	312.2	+ 0.2	B0 IaTp	6.2	-0.01	+0.27	11.6:	-	-	-	-	2
152723	312.5	+ 0.2	O6	7.0	-0.06	+0.23:	10.6:	1.2	.025	43::	94::	1
153426	314.9	+ 1.0	B2	7.5	-0.06	+0.17		2.3	.050	0°	52°	3
154040	314.4	- 0.1	B2e	10.0	+0.03	+0.26		0.8:	.017:	70	123	3
154090	318.6	+ 3.0	B1 Iab	4.9	-0.01	+0.23	10.0	-	-	-	-	2
154445	347.0	+21.4	B1 V	5.5	-0.11	+0.13	7.9	3.5	.077	88	147	4(3)
154450	317.5	+ 1.6	B0.5 IVp	8.7	+0.04	+0.29	10.9	0.6	.012	71	124	2
154911	315.5	- 0.4	B0e	9.2	+0.04	+0.30		1.6	.035	138°	11°	2
156134	318.9	0.0	B0 I	8.2	+0.16	+0.42	12.0	2.5	.054	117	172	2
156154	319.0	+ 0.1	O7	8.3	+0.13	+0.41	10.8	2.0	.044	123	178	2
156201	319.2	+ 0.1	B0	8.0	+0.20	+0.46		1.5	.033	124	179	2
158705	323.9	- 0.3	B0	8.1	+0.24	+0.50		1.8	.039	122	179	3

TABLE 2 (Continued)

HD	$\ell$	b	Sp	$m_v$	$C_1$	$E_1$	$m_0-M$	$P_g$	$P_{\Delta m}$	$\theta_E$	$\theta_G$	No.
159176*	323.3	- 1.3	O7	5.7	-.11	+.18	9.6	1.6	.034	163°	40°	4(3)
159975	344.8	+10.9	B8	4.6				0.8:	.018:	101:	160:	1
160529	323.4	- 3.1	A2 Ia+	6.7	+.48	+.56	10.3+	7.2	.156	18	76	5(3)
316197	328.5	- 0.5	B3 V	9.6	+.13	+.35	9.5	5.5	.120	174	52	2
161056	346.4	+10.1	B5n	9.2	+.05	+.24	9.0:	3.5	.077	66	126	3
161103	329.0	+ 0.4	B2:pe(III-IV)	8.5	+.07	+.30	10.4:	4.9	.106	170°	48°	5
316204	328.1	- 1.1	B2 III	9.2	+.02	+.25	11.8	4.0	.088	166	44	2
161291	329.2	- 0.6	B1 Iab	8.9	+.24	+.49	12.4	6.5	.142	1	59	3
161306	344.1	+ 8.5	B(O)ne	8.2	+.13	+.39		3.5	.075	64	124	3
316332*	327.3	- 2.1	B3 Ia	9.5	+.55	+.77	11.7	1.8	.040	15	74	2
316285	329.8	- 1.4	Beq					3.1	.068	162°	41°	2
161961	351.3	+11.4	B0.5 III	7.8	-.04	+.21	10.9	2.3	.050	74	135	2
162168	324.8	- 4.5	B0	8.5	+.15	+.41		2.5	.054	169	48	2
316415	328.0	- 2.6	B3	10.0	+.24	+.46		2.5	.054	3	63	1
162717	332.6	- 0.5	B3	9.2	+.17	+.39		3.0	.065	176	55	3
162718	332.0	- 0.8	B0ne	8.9	+.17	+.43		3.5	.076	0°	59°	2
162742	328.5	- 3.0	B3	8.4	+.06	+.28		2.7:	.058:	159°	38°	2
316569	327.9	- 3.5	B3 II	9.4	+.02	+.24	12.4	1.3	.028	11	71	2
316568	328.0	- 3.5	B2pe(IV-V)	9.7	+.01	+.24	11.2:	1.7	.038	8	68	2
162978	332.2	- 1.1	B2	6.2	-.14	+.09		1.2	.026	179	58	4(4)
163065	327.4	- 4.1	B1 Iab	8.6	+.05	+.29	13.3:	1.7	.038	38°	98°	1
163453	329.6	- 3.3	B0.5:pe(V)	9.3	+.18	+.43	10.3	2.0	.043	16	76	2
316730	328.3	- 4.2	B3	9.6	+.02	+.24		1.4:	.031:	169	49	1
164018	334.4	- 1.3	B3	9.3	+.18	+.40		1.4:	.031:	119:	179:	1
164019	329.6	- 4.0	B0 Ia:	9.3	-.03	+.23	14.9:	2.4	.052	177	57	1
164438	338.1	+ 0.3	O9 IV	7.2	+.02	+.29	10.2	1.0	.021	70°	130°	3
164536	333.7	- 2.4	B3	6.8	-.16	+.06		0.8	.018	153	33	4(3)
164906	333.7	- 2.8	B1 IV:pe	7.5	-.06	+.18	10.2	0.5	.010	-	-	2
164947	333.8	- 2.8	B5	8.4	-.11	+.08		0.8	.018	71	131	1
165052	333.8	- 2.9	O7	6.9	-.10	+.17	10.9	-	-	-	-	2
165517	333.4	- 3.7	Be	8.6	+.11	+.37		1.4:	.030:	44:	105:	3
165793	323.3	- 9.5	B0	6.6	-.17	+.09		1.0	.021	155	37	2
165998	336.5	- 2.4	B3	8.7	+.23	+.45		2.4	.052	81	142	2
166418	341.2	- 0.5	B0 II	8.1	+.07	+.33	11.3	3.0	.065	86	147	3(3)
166540	341.1	- 0.7	B0.5 IV	7.9	-.04	+.21	10.6	0.7	.016	70	131	3
168552	342.0	- 2.7	B3 Ib	8.2	+.04	+.26	12.3	0.4	.008	98°	160°	2
168571	341.8	- 2.9	B1 Ib - II	7.9	+.13	+.37	11.1	1.1	.024	94	156	2
169454	345.2	- 2.2	B 1 Ia+	6.7	+.29	+.53	10.5+	2.1	.045	16	78	3(3)
169827	342.5	- 4.1	B5	8.1	+.03	+.21		2.3	.050	115	177	1
170938	344.5	- 4.5	B1 Ia	7.9	+.28	+.52	11.7	3.8	.082	117	6	4(3)
171432	342.3	- 6.5	B1 Ia	7.0	-.03	+.21	12.7	1.8	.040	120°	2°	2
171589	346.4	- 4.6	O7 f	8.2	-.03	+.26	11.6:	0.8:	.017:	177:	59:	3
172252	348.7	- 4.3	B0 V:e	9.5	+.21	+.47	11.8	4.7	.102	148	30	2
172510	346.3	- 5.9	B1 V	8.7	-.02	+.22	10.6	2.6	.056	166	49	3
179406	356.0	- 9.8	B3n	5.3	-.04	+.18		1.6:	.035:	172	55	2



TABLE 2 (Continued)

HD	$l$	$b$	Sp	$m_v$	$C_1$	$E_1$	$m_o-M$	$P_{\%}$	$P_{\Delta m}$	$\theta_E$	$\theta_G$	No.
181615	349.6	-15.3	B8p + F2p	4.5				1.5:	.033:	166°	51°	2
183143	20.9	-0.5	B7 Ia	6.8	+.38	+.54	10.5	6.8	.147	0	60	2
184915	359.6	-14.7	B0.5 III	5.0	-.14	+.11	8.8	1.4:	.031:	165°	48°	4

TABLE 2. REMARKS

HD 298310	Classified as G in HDE; new classification on basis of ADH prism plates.
80077	Spectrum peculiar, consequently $E_1$ may be in error
92206	In H II region, No. 31 of Hoffleit's catalogue
92207	(1953) HD 92206 must be exciting star.
97950	Peculiar star, possibly very high luminosity excites H II region. Hoffleit No 57.
110432	Emission star, surrounded by cluster of faint stars. Assumed to be of luminosity class V for purposes of determining distance modulus.
311999	Exciting star of emission nebula lying beyond Coal Sack (Lindsay 1941; Houck unpublished)
134959	Surrounded by group of faint stars, some of which may have affected polarization measures.
159176	In galactic cluster NGC 6383, and excites H II region.
316332	Highly reddened star yet relatively small polarization. Hiltner (1954) has already drawn attention to this star.

where the line of sight traverses the Orion spiral arm, and here the alignment is most uniform and closely parallel to the galactic equator. This roughly confirms the hypothesis that the elongated polarizing particles are aligned perpendicular to the spiral-arm axis (Davis and Greenstein 1951; Hoag 1953). Such a model assumes that, in the ideal situation, the aligning force, presumably a magnetic field, orients the particles so that the maximum of the electric vector lies parallel to the spiral-arm axis. This hypothesis may be tested more definitively by mathematically relating interstellar polarization with spiral structure. The possibility that the magnetic field lies in a plane different from that of the galactic equatorial plane in some regions of the Milky Way cannot be entirely excluded on the basis of present data. The following discussion attempts to show that there is good evidence that the two planes are coincident over the greater part of the Milky Way and that the magnetic field is closely related to spiral structure.

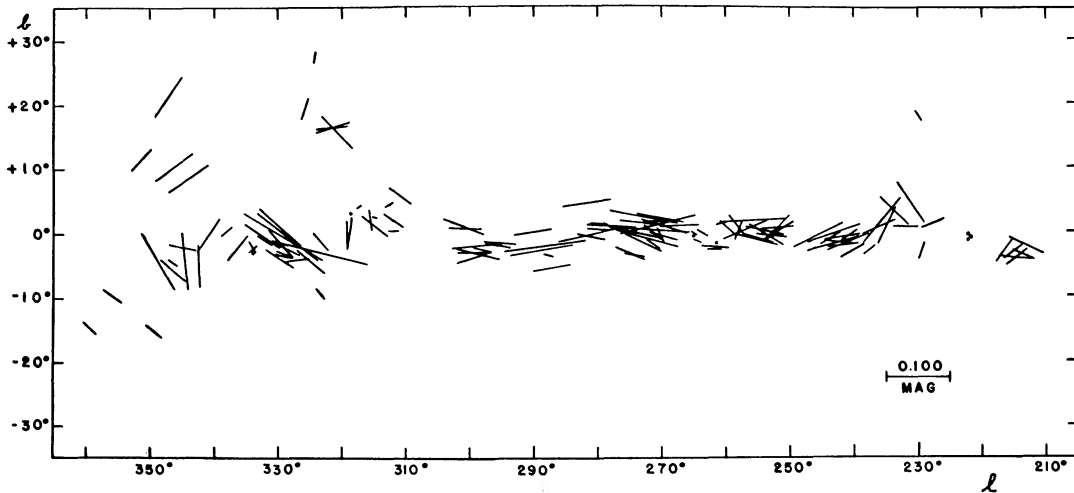


FIG 1—Interstellar polarization in the southern Milky Way. The direction is determined by the position angle of the plane of vibration, whereas the length of the line is proportional to the amount of polarization as indicated by the scale. Solid circles imply that the starlight suffers no or negligible polarization.

We shall follow a procedure similar to Hoag's (1953; unpublished).<sup>2</sup> First let us define the parameter

$$P^* = P_{\Delta m} (\sin \theta_G - \cos \theta_G), \quad (1)$$

where  $P_{\Delta m}$  is the observed amount of polarization in magnitudes and  $\theta_G$  is the position angle of the plane of vibration referred to the galactic co-ordinate system. We may further define  $E_{\max}$  as the maximum of the electric vector, described jointly by  $P$  and  $\theta_G$ . The difference between the orthogonal components of  $P_{\Delta m}$  serves as a measure of the collimation of  $E_{\max}$  in the galactic plane and strongly favors those  $E_{\max}$  which lie closely parallel to the galactic equator. For individual stars the value of  $P^*$  has relatively little significance; only when averaged over several stars is it meaningful. Thus the dispersion in position angle is inversely incorporated into  $P^*$ . Actually,  $P^*/A$ , the amount of polarization per unit absorption, represents the physically significant parameter, for it takes into account the dependence of polarization on the amount of extinction.

Supposing that the particles are aligned normal to the spiral-arm axis, we may predict that

$$\frac{P^*}{A} = k (1 - \cos \alpha), \quad (2)$$

<sup>2</sup> The following analysis resulted largely from private correspondence with Dr. A. A. Hoag, to whom I am much indebted.

where  $k$  is a constant of proportionality to be determined from the observations and  $\alpha$  is the angle between the axis of the arm and the line of sight. Obviously, for the Orion arm we may use the approximation

$$\cos \alpha = \sin |l - l_0|. \quad (3)$$

The galactic longitude of the region under consideration is given by  $l$ , whereas  $l_0$  denotes the longitude at which the arm lies perpendicular to the line of sight. Although  $l_0$  could be determined from our knowledge of spiral structure in the Galaxy, an independent method consists in plotting  $P^*/A$  as a function of longitude, as shown in Figure 2. The function  $P^*/A$  reaches a maximum at  $l_0 = 290^\circ$  in the south and  $125^\circ$  in the north. Similarly, the constant  $k$  derives from the slope of  $P^*/A$  plotted against  $(1 - \sin |l - l_0|)$ . Such graphs for both the southern and the northern hemisphere are given in

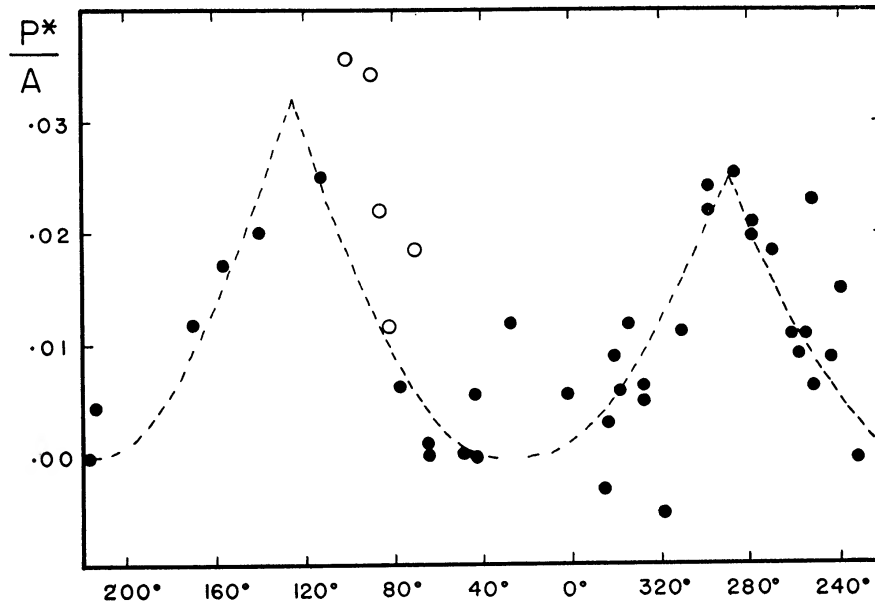


FIG. 2—Variation of the parameter  $P^*/A$  with galactic longitude. This parameter is defined in the text. Equations (4) describe the dotted curves. The solid circles are derived from data on associations probably lying in the Orion arm in the north and in the Sagittarius arm in the south. Open circles refer to data obtained for the Perseus arm aggregates.

Figure 3, from which we find  $k = 0.025$  and  $0.032$ , respectively. Therefore, equation (2) may now be written

$$\text{(South)} \quad \frac{P^*}{A} = 0.025 (1 - \sin |l - 290^\circ|), \quad (4a)$$

$$\text{(North)} \quad \frac{P^*}{A} = 0.032 (1 - \sin |l - 125^\circ|). \quad (4b)$$

The observational data used for this part of the analysis are those reported in the earlier portion of this paper for the Southern Hemisphere and those published by Hall and Mikesell (1950) and by Hiltner (1951) for the Northern Hemisphere. Each point in Figures 2 and 3 represents an aggregate or perhaps only a group of stars within a given region of space. Only stars in the Orion and Sagittarius arms were used for the southern data, while only Orion arm aggregates (Morgan, Whitford, and Code 1953)

entered into the analysis leading to equation (4b). Although the southern stars lie for the most part in the Sagittarius arm, much of the obscuring and polarizing matter is near the sun and constitutes part of the Orion arm. The Coal Sack and the Vela dark nebula, for instance, are at distances of approximately 150 and 500 pc from the sun, as determined from star-count analyses (Greenstein 1937; Lindsay 1941). In spite of considerable scatter, the observational data do satisfy equations (4).

Hence the model of a polarizing medium lying in the solar vicinity, with the particles aligned in planes normal to a given axis, seems to be roughly confirmed. We have assumed this axis to correspond to the axis of the Orion arm. The form of the curve in Figure 2 excludes the possibility that the axis is that of the Sagittarius arm. Since the Orion arm passes through the sun from approximately longitude  $210^\circ$  to  $30^\circ$ , one would expect  $l_0$  to occur at  $300^\circ$  and  $120^\circ$ , whereas actually the observations indicate  $l_0$  at  $290^\circ$  and  $125^\circ$ . The agreement is fair within the deviations due to local effects and uncertainties in the exact location of our spiral arm.

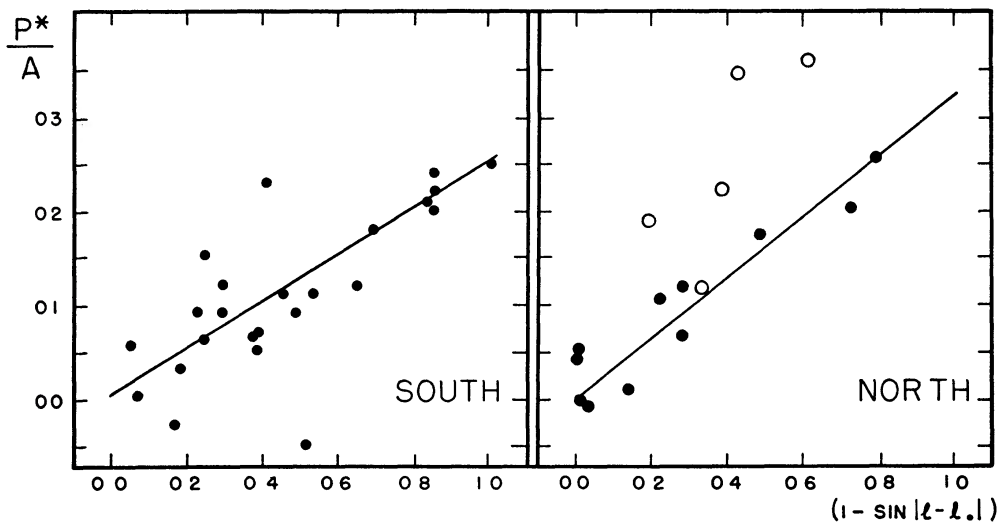


FIG. 3.—The parameter  $P^*/A$  plotted against  $(1 - \sin |l - l_0|)$ . The slopes of the lines are 0.025 and 0.032 for the south and north, respectively. See Fig. 2 for an explanation of the symbols used.

Whereas  $l_0$  depends solely on spiral structure in the vicinity of the sun, the constant  $k$  depends on the optical properties of the polarizing particles and on their degree of alignment. We must now consider how the difference in  $k$  between the northern and southern hemispheres may be explained. The discrepancy is even greater when Perseus arm associations are considered. These appear as open circles in Figures 2 and 3 and clearly have an even greater value of  $k$ , near 0.06, than the northern Orion arm aggregates, with  $k = 0.032$ . One might attribute the discrepancy to a difference in the optical properties of the grains. This seems hardly likely, as the extinction properties could then also be expected to differ appreciably. Although there is some evidence for slight differences in the interstellar reddening law (Johnson and Morgan 1955), they are small, and considerable evidence points to a generally homogeneous medium if peculiarities due to excited nebulae are ignored (Stebbins and Whitford 1945; Divan 1955; Houck 1955).

The factor  $P/A$  is perhaps a more convincing parameter, as it does not include the cosine factor involved in  $P^*/A$  and therefore does not depend on the model of the polarizing medium. An examination of the data for the southern and northern observations indicates that  $P/A$  varies with longitude in the same general manner as  $P^*/A$ , though the scatter is greater. The difference between the northern and southern data exists for  $P/A$  as well as for  $P^*/A$  and therefore appears to be real.

The second contributing factor is the degree of alignment. We tentatively suggest that the difference is due to a concentration of the aligning force, probably a magnetic field, toward the central axis of a spiral arm. Such a concentration would result in the elongated particles' being less rigidly aligned at the periphery of an arm than at its center. Consequently, the value of  $k$  should be lower at the edge of an arm. Studies of spiral structure in the solar neighborhood (Morgan, Whitford, and Code 1953; van de Hulst, Muller, and Oort 1954) indicate that the sun is located near the edge of the Orion arm nearest the galactic center. If we look southward, therefore, the line of sight passes through only an outer section of the arm, whereas northward it crosses the center. The difference in the values of  $k$  thus conforms to our hypothesis.

The Perseus arm data may represent an aspect of the same phenomenon. Not too great weight can be given to distance determinations by star counts, but such analyses do indicate that the obscuring clouds in this field lie within our own arm (Wernberg

TABLE 3  
DATA ON INDIVIDUAL REGIONS

Region	$l$	$b$	$\bar{\theta}_G$	$\sigma_\theta$	$P/A$	$P^*/A$	$\overline{m_0 - M}$	No. Stars
Vela	241°	-1°1	106°	14 4	0 020	+0 015	11 6	10
Carina (1)	252	+0 4	120	11 7	015	+ 006	11 7	5
NGC 3293	253	+0 2	90	13 0	028	+ 023	11 9	7
$\eta$ Carinae	255	-0 8	70	14 0	018	.	.	6
Carina (2)	257	+0 5	101	32 7	020	+ 011	11 8	8
Carina (3)	259	+1 4	74	21 5	016	+ 009	12 6	4
Centaurus (1)	263	-1 1	74	15 0	015	+ 011	12 1	6
Coal Sack	272	0	81	10 8	021	+ 018	11 7	14
Coal Sack	272	>0	87	10 2	026	.	.	20
Coal Sack	272	<0	67	15 8	017	.	.	14
Centaurus (2)	281	-0 5	86	9 4	024	+ 020	..	8
Circinus	288	-2 6	91	13 0	030	+ 025	10.9::	3
Norma	299	-3 0	89	7 6	026	+ 024	11?	5
NGC 6231	311	+0 2	88	8 2	009	+ 008	10 6	4
Scorpius	319	+1	..	..	010	- 007	..	5
Sagittarius	328	-2 1	59	14 9	0 022	+0 006	..	18

1941; Heeschen 1951). None of the Orion arm associations considered previously lie in the same field as the Perseus aggregates, so a direct comparison is not possible. The spread in position angle for Perseus aggregates is lower than in most other parts of the Milky Way. Perhaps we are dealing with a cloud or complex whose particles are better aligned than in the general case because it happens to lie near the center of the arm, where the aligning force reaches its greatest strength. In most regions such an ideal situation does not exist because several clouds are involved, some of which may be at some distance from the central axis. Unfortunately, knowledge of distances of dark nebulae are too scant and uncertain for us to test this hypothesis very critically.

Observations of stars whose light might be polarized by interstellar clouds lying in either the Sagittarius or the Perseus arm are too few to enable us to study the polarizing medium in these spiral arms. Clouds in the Orion arm would also influence the polarization and complicate the analysis.

#### IV. INDIVIDUAL REGIONS OF SPECIAL INTEREST IN SOUTHERN MILKY WAY

Table 3 summarizes the important characteristics of the various regions. For convenience, numbers are given in parentheses after the constellation name when more than one group of stars lies in a given region. Some of these groups may form associations or

be members of associations, since the stars are grouped according to distance modulus as well as field. An extension of the Morgan, Whitford, and Code paper (1953) assigning Roman numerals to aggregates in the southern Milky Way will probably result from the work of the Washburn South African Expedition. Arabic rather than Roman numerals are used here, to avoid confusion at a later time.

The dispersion in position angle,  $\sigma_\theta$ , serves as a rough indication of the degree of parallelism for the planes of vibration of the polarized light from the several stars in a given group. Since the sample of data leading to each  $\sigma_\theta$  is small, the tabulated quantities carry small weight. A more reliable parameter is  $P^*/A$ , discussed previously, which may be defined as the amount of polarization per unit absorption parallel to the galactic equator.

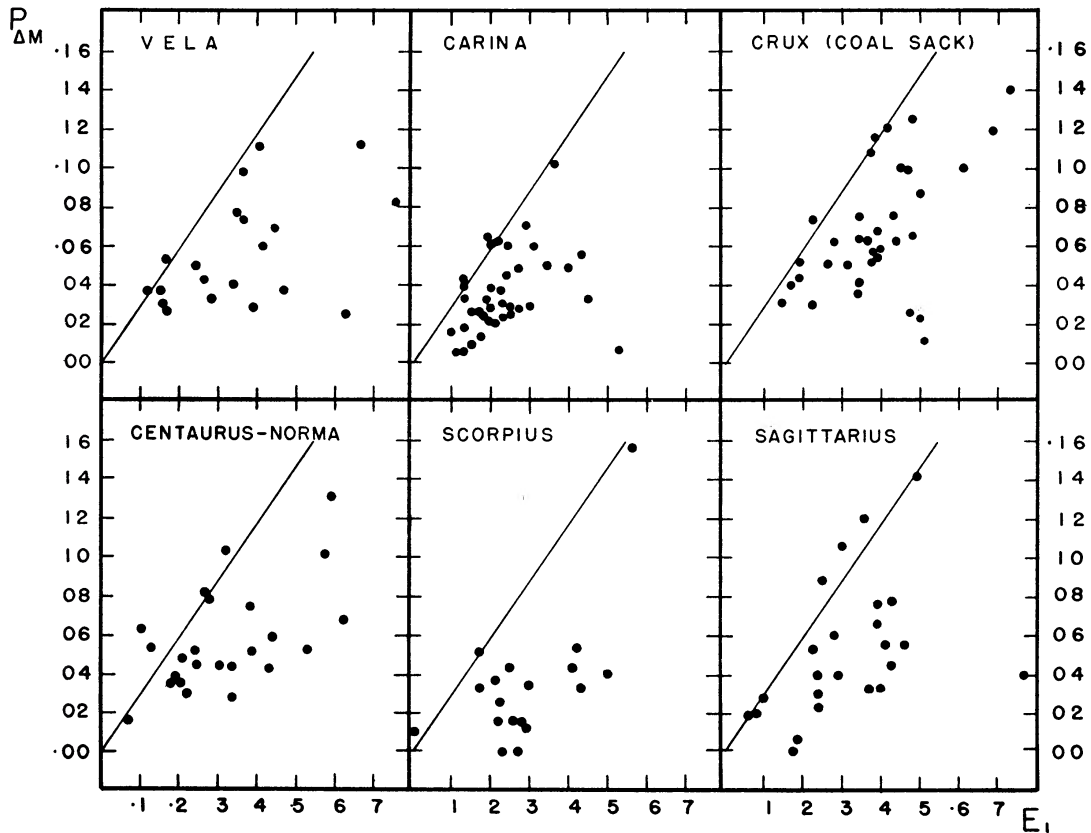


FIG. 4—Relation between polarization and color excess. The line is defined by relation (5) in the text.

The relation between polarization and color excess for the several regions is shown in Figure 4. The relation

$$P_{\Delta m} = 0.34E_1 \quad (5)$$

represents the maximum ratio of polarization to color excess and defines the line drawn in each diagram. A few points lie above this line, since the relation is actually derived from the several highest ratios observed. The scatter is considerable in all cases but varies from one region to the next, as does the percentage of stars lying near the maximum slope.

*Vela*

Present data on spiral structure, though still meager, suggest that the direction of longitude  $240^\circ$  points between the Orion and Sagittarius arms. A streamer may possibly exist connecting the two arms at a distance of about 1.5–2 kpc from the sun and extending from  $220^\circ$  to  $240^\circ$ . Several members of an OB association at  $l = 240^\circ$  and at 2 kpc (Houck, unpublished) were observed for polarization. The Vela dark nebula (Greenstein 1937), lying at approximately 500 pc and therefore part of the sun's spiral arm, probably contributes most of the reddening and polarization. The patchy distribution of the amounts of polarization and absorption may be seen in Figure 5, wherein the radii of the circles are proportional to the absorption.

*Carina*

The Carina region is highly complex; here the stars observed probably lie in that part of the Sagittarius arm where it curves away from us along the line of sight. For the most

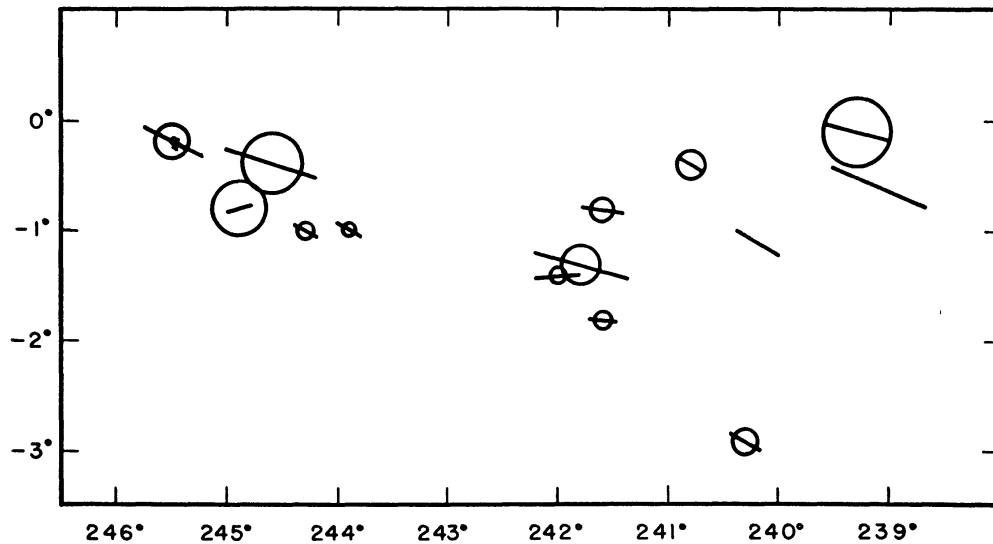


FIG 5—Polarization in Vela. The figure portrays the projected space distribution of the maximum of the electric vector in the Vela region. The radii of the circles are proportional to the color excesses.

part, the absorption does not exceed 2 mag. This is one of the few regions where the obscuring clouds may be in the Sagittarius and not in the Orion arm (Bok 1937). Perhaps the scatter of the points in the plot of  $P^*/A$  against longitude (Fig. 2) at  $l \sim 255^\circ$  may result from the fact that some of the absorption occurs in the Orion arm and some in the Sagittarius arm. Figure 6 illustrates the polarization in the Carina region projected on the star field. The group at  $l = 252^\circ$ , Carina (1), which may form an aggregate at 2.2 kpc, has rather low polarization in comparison with the color excess, but the dispersion in position angle,  $12^\circ$ , is quite low.

The galactic cluster, NGC 3293 at  $l = 253^\circ$ ,  $b = +0.2^\circ$ , and at a distance of about 2.3 kpc, may be associated with the afore-mentioned aggregate. An H II region, No. 26 in Hoffleit's catalogue (1953), lies near the cluster, but it is difficult to relate the observed polarization with direction of the wisps or streamers of the nebulosity. Several stars in or superposed on the  $\eta$  Carinae nebula were also observed for polarization, as shown in Figure 6.

The stars near  $l = 258^\circ$  are separated into two distinct groups, Carina (2) and (3), on the basis of their respective distances. The more distant group is the less reddened, per-

haps because of the irregularity of the absorbing medium. Possibly the general disorder of the polarization in the region as a whole may be ascribed to the inhomogeneity of the interstellar clouds. Bok and van Wijk (1952) have already commented on the patchiness of the obscuration in this locality.

#### *The Coal Sack*

The Coal Sack in Crux gives the appearance of a fairly uniform, compact dust cloud. Star counts indicate that it is at a distance of about 150 pc (Unsöld 1929; Lindsay 1941), which places it in the sun's spiral arm. Absorptions ranging from 1 to 3 mag. are similarly derived from star counts. Analysis of reddening data correlated with distances gives a somewhat complex picture. The highest obscuration occurs in the neighborhood of  $l = 271^{\circ}5$ ,  $b = +1^{\circ}0$ , and diminishes irregularly outward from this center. In the southern part of the nebula the absorption is not quite so high as in the northern section, but direct photographs suggest that it is also less uniform. An OB aggregate happens to lie well behind the Coal Sack ( $m_0 - M = 11.7$ ,  $r = 2.2$  kpc) but in the same line of sight (Houck, unpublished). Magnitudes and colors are known for nearly all the stars I observed, and MK spectral types for a great many (Houck, unpublished); so many available data make possible a fairly detailed study of the region. Nevertheless, we still lack a quantitative picture of the distribution of the absorbing medium.

Unfortunately, even the brightest of the stars observed lie well beyond the Coal Sack, so we can make no comparison between stars in front of and behind the dust cloud. The stars at distances of less than 2 kpc are not highly reddened, but fortuitously they are all situated at the periphery of the cloud, where the absorption is less. The polarization characteristics for these stars are quite comparable to those for the members of the aggregate. The uniformity of the polarization characteristics suggests that, even for the more distant stars, the Coal Sack is the predominant dust cloud.

In regard to distance effects, then, we may consider the Coal Sack as a unified region. A glance at Figure 7, however, shows that both polarization and absorption differ between the northern and southern portions. Let us take  $b = 0^{\circ}$  as the dividing line and find the quantitative polarization characteristics for the two fields. The results are incorporated in Table 3, in addition to those for the Coal Sack aggregate proper. Not only is the deviation of the position angle in the southern half higher than in the northern, but the means of the angles differ by  $20^{\circ}$ , with the planes of vibration in the north being more closely parallel to the galactic equator than in the south. We note further that the ratio of polarization to absorption for the north considerably exceeds that in the south. Local structure within the nebula must surely cause this disparity; perhaps there are several small clouds rather than one uniform one. The peculiar motions of these clouds may either directly align the particles differently or distort the magnetic field, which in turn causes the grains to become preferentially oriented in divergent directions. The irregular structure in the south suggests that here the cloud is broken up into smaller units than in the north.

#### *Centaurus to Sagittarius*

The Milky Way from  $l = 280^{\circ}$  to  $l = 310^{\circ}$  is heavily obscured by complex dark nebulae (Bok 1937; Code and Houck 1955). Not many early-type stars are known in this region, probably because of the overlying absorption. Table 3 summarizes the results of polarization measurements in this longitude interval. Stars used in compiling these data were selected on the basis of probable membership in the Sagittarius arm. This selection necessitated some guesswork relative to distance moduli for those stars whose spectral type on the MK system was unknown. The observational data satisfy fairly well the polarization model already discussed.

At  $l = 311^{\circ}$  in Scorpius we have the cluster NGC 6231 and the associated aggregate (Morgan, González, and González 1953). Although the absorption is not exceptionally



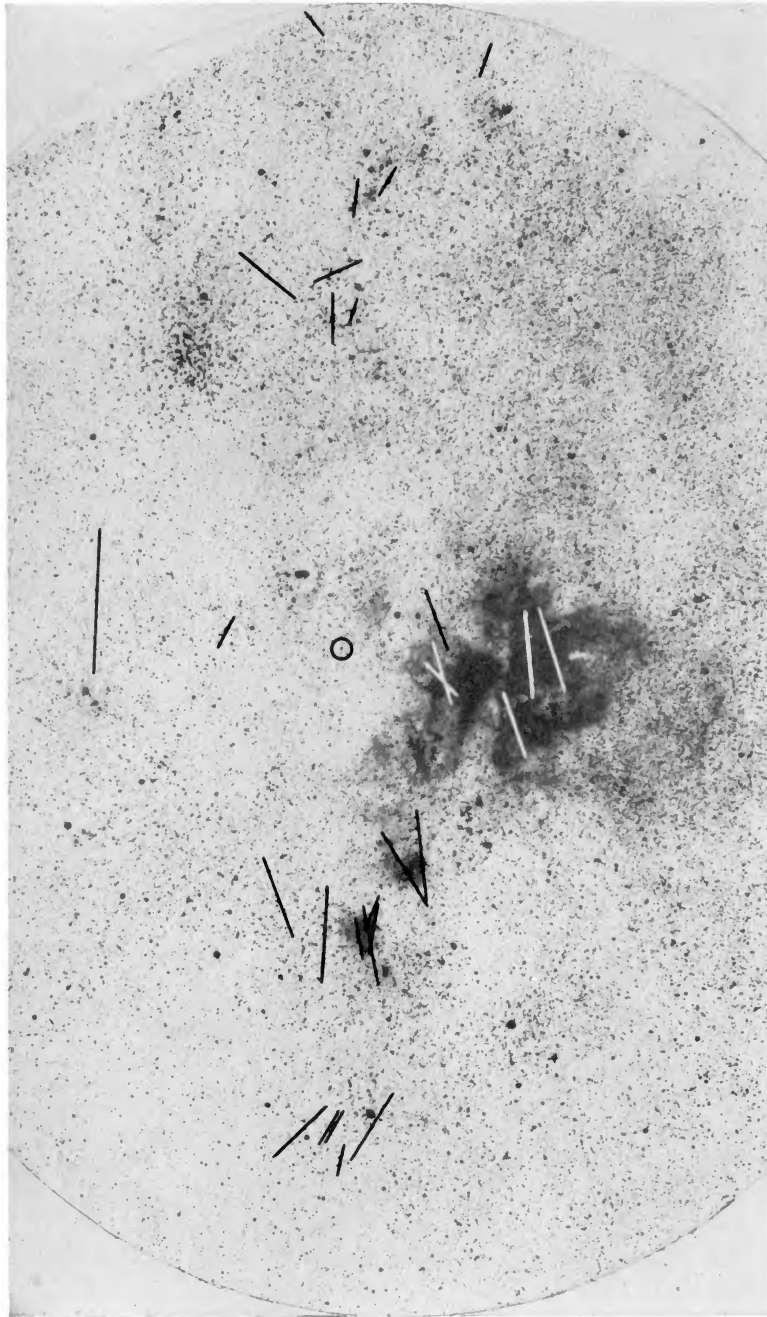


Fig. 6.—Polarization in Carina projected on the star field. The  $\eta$  Carinae nebula appears near the center of the plate; NGC 3293 lies to the west, namely, on the left. The lower edge of the plate lies parallel to the galactic equator.

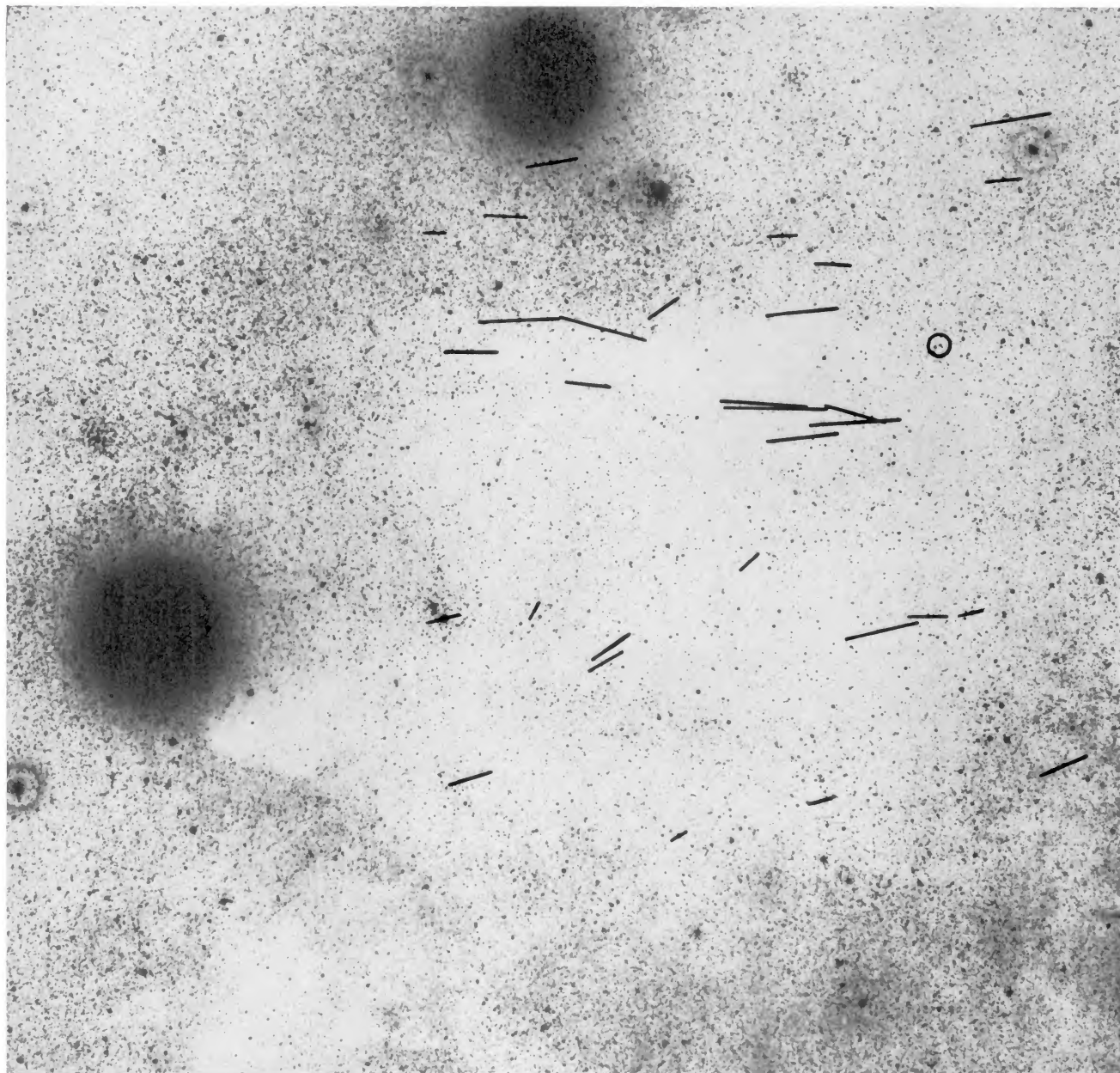


FIG. 7.—Polarization in the Coal Sack. The lower edge of the plate lies parallel to the galactic equator, which runs closely through the middle. East is on the right.

high, it is not negligible; yet the polarization for all stars observed is very low. The resulting  $P^*/A$  for the region lies far below the predicted value. This state of affairs continues as we proceed to greater longitudes, as illustrated in Figure 8. The obscuration here also is exceedingly complex and patchy, giving the appearance, in fact, of turbulence. Photographs taken in  $H\alpha$  light indicate that the hydrogen emission also has a very turbulent appearance (Bok 1955), which suggests that both gas and dust are irregularly distributed. The situation may be comparable to that suggested for the southern section of the Coal Sack: several small clouds making up a big complex, whose motion is directly or indirectly responsible for the disorder in the alignment of the particles.

In Sagittarius the obscuration increases still further but remains very irregular. Many cases of high polarization exist, but the planes of vibration lie at considerable angles relative to the galactic equator, making  $P^*/A$  close to zero in spite of the fact that  $P/A$  is high. Many of the stars observed have also been studied by Hall and Mikesell (1950) and by Hiltner (1951, 1954).

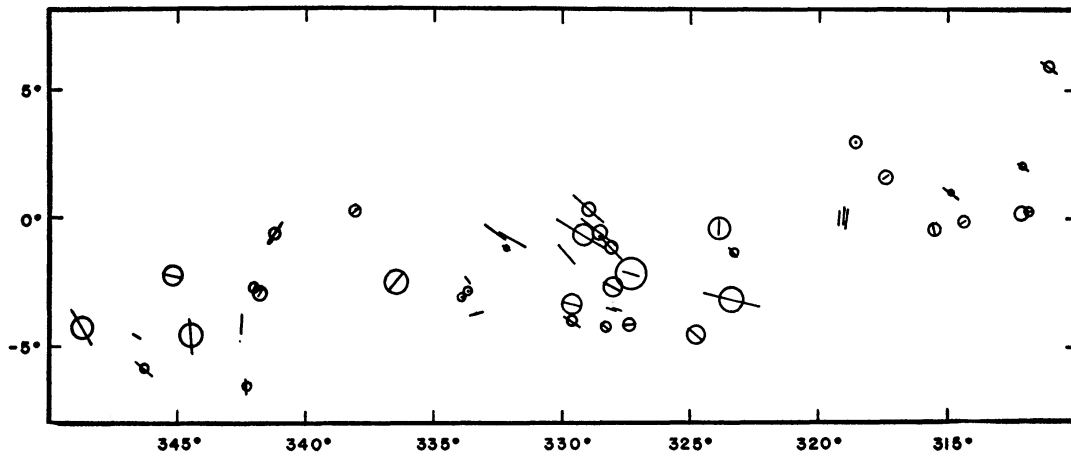


FIG. 8—Polarization and color excess in Scorpius-Sagittarius

Disorder is the predominant characteristic of the polarization at greater longitudes, which is to be expected from the polarization model. From South Africa I observed only a few stars in this region, which had already been covered from the north. Figure 8 includes these observations, to illustrate the general trend.

#### V. CONCLUSION

We have seen that polarization measurements relate well to spiral structure if we envisage the polarization as caused by grains which are preferentially aligned perpendicular to the spiral-arm axis. Nevertheless, aberrations due to local structure may be quite severe, as in the Scorpius region. The data available at present allow us to study the polarizing medium within our own spiral arm, the Orion arm. Future observations should concentrate on aggregates in the more distant spiral arms, such as the one beyond Perseus and the second inner arm. A few scattered observations of this type already exist but are insufficient to provide a clear general picture.

Finally, I should like to express my appreciation to the many persons who have aided me in the course of this work. In particular, I am grateful to the Harvard Observatory Council for the opportunity to observe at the Boyden Station. I am indebted to R. B. Dunn, who contributed generously to the design and construction of the polarimeter used on the 60-inch telescope. T. E. Houck and the Washburn Observatory were most

generous in allowing me the use of some of their equipment and in supplying me with data prior to publication. My special thanks go to Drs. B. J. Bok and J. S. Hall, who gave me much of their time, advice, and encouragement.

## REFERENCES

- Bok, B. J. 1937, *The Distribution of the Stars in Space* (Chicago: University of Chicago Press), pp 82 ff.  
 ———. 1955, *A J*, **60**, 146  
 Bok, B. J., and van Wijk, U 1952, *A J*, **57**, 213  
 Code, A. D., and Houck, T. E. 1955, *Ap J*, **121**, 553.  
 Davis, L., and Greenstein, J. L. 1951, *Ap J*, **114**, 206.  
 Divan, L. 1954, *Ann. d'ap*, **17**, 456  
 Greenstein, J. L. 1937, *Harvard Ann*, **105**, 359  
 Hall, J. S., and Mikesell, A. H. 1950, *Pub U S Naval Obs*, Vol **17**, Part I  
 Heesch, D. S. 1951, *Ap J*, **114**, 132  
 Hiltner, W. A. 1951, *Ap J*, **114**, 241  
 ———. 1954, *ibid*, **120**, 41  
 Hoag, A. A. 1953, *A J*, **58**, 42.  
 Hoffleit, D. 1953, *Harvard Ann*, Vol. **119**, No. 2  
 Houck, T. E. 1955, private communication  
 Hulst, H. C. van de, Muller, C. A., and Oort, J. H. 1954, *B A N*, **12**, 117.  
 Jackson, J., and Stoy, R. H. 1954, *Ann Cape Obs*, Vol **17**  
 ———. 1955, *ibid*, Vol **18**.  
 Johnson, H. L., and Morgan, W. W. 1951, *Ap J*, **114**, 522.  
 ———. 1953, *ibid*, **117**, 313  
 ———. 1955, *ibid*, **122**, 142.  
 Lindsay, E. M. 1941, *Proc Roy Irish Acad., A*, Vol. **46**, No. 11.  
 Morgan, W. W., Code, A. D., and Whitford, A. E. 1955, *Ap J Suppl*, **2**, 41 (No. 14)  
 Morgan, W. W., González, G., and González, G. 1953, *Ap J*, **118**, 323  
 Morgan, W. W., Harris, D. L., and Johnson, H. L., 1953, *Ap J*, **118**, 92  
 Morgan, W. W., and Keenan, P. C. 1951, *Astrophysics*, ed Hynek (New York: McGraw-Hill Book Co.),  
 chap i  
 Morgan, W. W., Whitford, A. E., and Code, A. D. 1953, *Ap J*, **118**, 318  
 Ohlson, J. 1932, *Ann Obs Lund*, No. 3.  
 Oosterhoff, P. T. 1951, *B A N*, **11**, 299  
 Sharpless, S. 1952, *Ap J*, **116**, 251  
 Stebbins, J., Huffer, C. M., and Whitford, A. E. 1940, *Ap J*, **91**, 20  
 Stebbins, J., and Whitford, A. E. 1945, *Ap J*, **102**, 318  
 Unsöld, A. 1929, *Harvard Bull.*, No. 870  
 Wernberg, G. 1941, *Uppsala Ann*, Vol **1**, No. 4.